Energy Reports 8 (2022) 3244–3250

Contents lists available at ScienceDirect

Energy Reports

journal homepage: www.elsevier.com/locate/egyr

Research paper

Bio-inspired blades with local trailing edge flexibility increase the efficiency of vertical axis wind turbines

M. Somoano [a], F.J. Huera-Huarte [b,*]

[a] IHCantabria - Instituto de Hidráulica Ambiental de la Universidad de Cantabria, 39011 Santander, Spain
[b] Department of Mechanical Engineering, Universitat Rovira i Virgili (URV), 43007 Tarragona, Spain

ARTICLE INFO

Article history:
Received 28 September 2021
Received in revised form 31 January 2022
Accepted 13 February 2022
Available online 25 February 2022

Keywords:
Cross-flow turbine
Vertical axis wind turbine
Vertical axis hydrokinetic turbine
Darrieus turbine
Trailing edge
Flexible blade

ABSTRACT

This experimental study is focused on quantifying the effect of trailing edge flexibility on the performance of a three straight bladed vertical axis wind turbine, with a chord-to-diameter ratio $c/D = 0.16$ at a moderately high Reynolds number (based on diameter) $Re_D = 4{\cdot}10^5$. The blades consist of NACA-0015 profiles that are fixed with a pitch angle $\beta = 6°$ toe-out, and allow interchangeable trailing edges in the last 17% of their chord length. The research presented here provides a proof of concept for the improved performance of vertical axis wind turbines, due to the effect of flexibility at the trailing edge of their blades. We show that blades with semi-flexible trailing edge, can extend the range of rotor operating regimes, leading to an increase of approximately 10% in the performance of the turbine. An excess of flexibility results in diminished efficiencies.

1. Introduction

Cross-flow turbines (CFTs) are often used to harvest kinetic energy from wind or water currents. They are characterised by having their rotating shaft perpendicular to the flow as opposed to axial-flow turbines (AFTs). In the field of wind engineering they are commonly known as vertical axis wind turbines (VAWTs) or Darrieus turbines (Darrieus, 1931). They have become increasingly popular in the last decades because of their compact size, a fact that makes them suitable for applications in urban environments. Despite the fact that they are known to have characteristics such as omni-directionality, lower manufacturing and maintenance costs, low noise emittance, and good behaviour at high wind velocities and in turbulent wind flows (Du et al., 2019a), they are not as extended in use as horizontal axis wind turbines (HAWTs). Recently, there has been an increased research interest in understanding the complex flow phenomena inside CFT rotors and how this is related to their performance. Ferrer and Willden (2015) used numerical techniques to study the blade-wake interactions that took place inside this type of rotors, as a function of the operational tip speed ratio (λ), defined as

$$\lambda = \frac{\omega D}{2u_\infty} \tag{1}$$

where ω is the rotational speed, D the turbine diameter and u_∞ the free stream velocity.

Somoano and Huera-Huarte (2017) studied experimentally the flow dynamics inside and around the rotor of a three straight-bladed CFT model, using planar digital particle image velocimetry (DPIV). The investigation allowed the authors to analyse how the vorticity generated in the upstream region of the turbine interacted with the downstream one. At low tip speed ratios, they showed that the wake was dominated by the free stream, promoting a local flow with significant radial component in the downstroke part of the rotor. For intermediate λ, the flow interactions around the blade in the downstroke region resulted in local velocity vectors with larger tangential components. At high tip speed ratios, the local wake of each blade was dominated by the rotational motion, implying a small lift component. Other authors (Li et al., 2014; Du et al., 2019b) recently used on-board pressure measurements to obtain the instantaneous pressure distribution around the blade during turbine operation. They were able to study flow derived phenomena including dynamic stall, laminar separation bubbles and vortex convection along the blade. Somoano and Huera-Huarte (2019) analysed experimentally in a water channel the variations in the flow dynamics and the blade–wake interactions inside the rotor of a CFT model for different pre-set blade pitches (β) in the range from 8° toe-in to 16° toe-out. DPIV results showed how small variations in β had enormous influence on the dynamic stall characteristics of the system. The angle of attack seen by the blade in the upstream part of the turbine depends on this β, and so does the timing of the leading-edge vortex (LEV) shedding, crucial for how the blade–wake interactions took place in the downstroke region. For a pitch angle near 8° toe-out, the LEV travelled closer

* Corresponding author.
E-mail address: francisco.huera@urv.cat (F.J. Huera-Huarte).

https://doi.org/10.1016/j.egyr.2022.02.151

to the blade, suggesting a constructive flow interaction. These larger forces on the blade in the downstroke part of the rotor for pitch angles in the range from 4° to 8° toe-out, were later confirmed by Somoano and Huera-Huarte (2018). The authors carried out experiments in a wind tunnel facility with a three straight-bladed CFT model, having the same blade profile and chord-to-diameter ratio (c/D), thus the same solidity ($\sigma = \frac{Nc}{\pi D}$), in order to study the combined effect of blade pitch and Reynolds number based on diameter ($Re_D = \frac{u_\infty D}{\nu}$, with ν being the fluid kinematic viscosity) in the range from $3 \cdot 10^5$ to $5 \cdot 10^5$.

Re_D is used in the present work to represent global effects on the turbine (Fujisawa and Shibuya, 2001; Bachant and Wosnik, 2014; Araya and Dabiri, 2015), instead of those related to local flow features when using c as the characteristic length. Efficiency is shown using performance curves, with the power coefficient as a function of λ. The power coefficient (C_P) is the ratio of the mechanical power in the shaft upon the power available in the free stream,

$$C_P = \frac{T\omega}{\frac{1}{2}\rho u_\infty^3 LD} \tag{2}$$

where T is the net torque applied on the shaft, ρ the fluid density and L the blade span. In the case of cross-flow turbines, the shape of the performance curve presents three well-defined regions as a function of tip speed ratio. At low and high λ, the efficiency of this type of rotors is lower than for intermediate tip speed ratios, where the C_P reaches its maximum values (Fiedler and Tullis, 2009; Li et al., 2016; Bachant and Wosnik, 2016; Strom et al., 2018). At the diameter Reynolds number $Re_D = 4 \cdot 10^5$, Somoano and Huera-Huarte (2018) showed how the dead band region (Baker, 1983) disappeared for $\beta = 6°$ toe-out. Thus, the net aerodynamic torque produced at the blades was higher than the resistive torque at all times, not only maximising rotor performance, but also self-starting from rest. The self-starting capabilities of this type of turbines is a well known issue (Dominy et al., 2007; Hill et al., 2008; Satrio and Utama, 2021). Mazarbhuiya et al. (2020) numerically found out that the optimal pitch for their asymmetric-bladed VAWT was 5° toe-out, showing that this toe-out angle improved the turbine performance in the upwind position, whereas a 5° toe-in angle augmented the turbine performance in the downwind part. This is in agreement with the results shown by Rezaeiha et al. (2017) and Du et al. (2019c), as the toe-out pitch reduces the angle of attack in the upstream half part of the rotor, delaying the blade dynamic stall that leads to the blade producing torque over a larger part of the cycle.

Several authors have suggested that the aerodynamic performance of flapping devices can be enhanced by using flexible wings (Dudley, 2000). This is inspired in the ability of nature's flyers and swimmers in controlling vorticity. Gerontakos and Lee (2008) showed that a downward trailing edge flap deflection on a rigid NACA-0015 aerofoil induced positive camber effects, leading to an increase in the strength of the detached leading edge vortices, enhancing lift. Worasinchai et al. (2012) investigated the self-starting capabilities of VAWTs, suggesting that the flow physics experienced by the blade in rotor motion, was analogous to that of a flapping wing mechanism. Recently, the case of an actuated tip in a flapping foil for bio-inspired propulsion was studied by Huera-Huarte and Gharib (2017, 2019), who showed that large changes in performance could be achieved by actuating the very last part of the foil. A similar configuration based on a flexible pitching foil was studied in detail by Huera-Huarte (2018), showing the positive effects of moderate flexibility in terms of impulse generation due to vortex timing and formation.

Simulations of an oscillating foil for energy harvesting using prescribed deformations (Liu et al., 2013), showed a remarkable increase in the local angle of attack, that led to enhanced efficiencies. The performance was largely conditioned by the flexibility of the oscillating foil. Liu et al. (2016) investigated the dynamics of a flapping foil energy harvester with a passively deformable foil. Their simulation results showed that the passive deformations of the trailing edge promoted the strength of the LEVs, leading to an increase of the overall energy extraction performance.

The use of flexible blades in axial-flow turbines is not scarce in the literature. Barber et al. (2017) studied in a flume, adaptative pitch-to-stall composite blades that twisted towards stall with increased fluid loading, decreasing the pitch angle and increasing the effective angle of attack. The authors showed how these passive-adaptative pitch blades increased power generation at low dimensional loads, but caused excessive out of plane deformation under higher loading conditions, resulting in loss of performance and ultimately in blade failure. Cognet et al. (2017) studied the effects of variations in the rigidity of the blades of a small scale axial flow turbine in wind tunnel experiments, by using plastic sheets with different rigidities. They reported increases in turbine performance in cases with semi-flexible blades. The performance enhancement was found to be governed by the fluid–structure interaction mechanism, in which the complex unsteady pressure loads acting on the blade, tended to bend it towards the headwind direction increasing the apparent pitch angle, and the centrifugal force acted to unfold the blade in the opposite direction. The blade passive reconfiguration resulting from this interaction, enhanced the performance of the machine, when flexibility was within a certain range. There is, however, a need for more research related to blade flexibility for the case of VAWT or CFT configurations with rotating blades characterised by blade-wake interactions. The idea of a blade having flexibility has been previously explored using simulations, in a CFT with high solidity by Bouzaher et al. (2017). Numerical simulations conducted by Wang et al. (2016) in a cross-flow turbine whose blade shape changed automatically into a desired geometry according to its surface pressure, showed improved power coefficients C_P at low rotor solidity. Baghdadi et al. (2020) demonstrated higher power output in a Darrieus turbine when blades were dynamically morphed to an optimised shape, which was a function of the azimuthal angle and the tip speed ratio. MacPhee and Beyene (2016) simulated a flexible bladed (or morphing) CFT by passive pitch control, achieving higher efficiency and suggesting the increase of self-starting capabilities. Zeiner-Gundersen (2015) confirmed the effectiveness of using a flexible foil CFT, with high solidity at low inflow water velocities. They used a passive pitch system that consisted of a pivoting spring-loaded mechanism in double-cambered blades.

The objective of the present work is to evaluate for the first time, the effect of the flexibility of the blade trailing-edge of a cross-flow turbine on its performance. To our knowledge, there are not published works devoted to the study of the implications of adopting flexibility only at the trailing edge of the blades, and how this modifies the performance of cross-flow turbines. The research presented here provides a proof of concept for the improved performance of vertical axis wind turbines, due to the effect of flexibility at the trailing edge of their blades. The concept is based on the previous work by Huera-Huarte and Gharib (2017, 2019), where the same idea was investigated but in that case, for bio-inspired propulsion. Here, a modular blade that allowed us to test different rigidities at the trailing edge, has been specifically designed for these experiments and tested in a wind tunnel. From the practical point of view, and in terms of blade construction and reliability, applying flexibility only at the trailing edge, can have important advantages when compared to having flexibility along the whole blade chord. By reducing flexural stiffness locally at the trailing edge, we expect the blade to reconfigure according to the

unsteady aerodynamic loading effects, self adapting to the flow, without compromising structural integrity as flexibility applies only at a small part of the blade. Nevertheless, further work is necessary to study the commercial applicability of the concept.

In the next part of the document (Section 2), the details of the experimental set-up are described. It continues with Section 3, where the main results and their discussion are presented, followed by the conclusions in Section 4.

2. Experimental set-up

The experiments were conducted with a three straight bladed cross-flow turbine model, with a rotor of diameter $D = 0.75$ m, which was mounted on a stainless-steel shaft with a diameter of 25 mm. The shaft was horizontally supported by two air bearings to ensure negligible dry friction losses when rotating. The three blades were 3D-printed in polylactic acid (PLA), based on a NACA-0015 profile with a chord $c = 0.12$ m and a span $L = 0.75$ m, leading to an aspect ratio of $L/c = 6.25$ as well as chord (c/D) and span (L/D) ratios of 0.16 and 1, respectively. Blades were reinforced internally with an 8 mm aluminium square tube to increase their span-wise rigidity. Two aluminium struts connected each blade inner core to the rotor shaft. The struts were located at 1/5 and 4/5 of the blade span and included 3D-printed parts that allowed to set up the desired fixed pitch angle of the blades. For the experiments, an angle of 6° toe-out was fixed. Note that a forward shift of the mount-point from the centre of the chord towards the leading edge corresponds to an effective toe-in pitch change of,

$$\beta = tan^{-1}\left(\frac{2x}{D}\right) \tag{3}$$

where x is the distance between these two points along the blade chord (Fiedler and Tullis, 2009). For these experiments, blades were especially designed to be modular, in a way that the last part of the blade, near the trailing edge could be easily changed. This last part of the blade with length c_t, yielded a tip to chord ratio of $c_t/c = 0.17$, inspired by the experiments carried out by Huera-Huarte and Gharib (2017, 2019), where an active tip control strategy was used for studying bio-inspired propulsion.

The flexible trailing-edges considered in the study, were made of calibrated brass sheets of different flexural stiffness, modulated by their thickness (e). A total of 4 rigidities were investigated, given by thickness of 100, 250, 400 and 500 μm. The design of the blade and the attachment of the sheets to the rigid part of the profile, allows only chord-wise flexibility near the trailing edge, deformations or twist are not allowed span-wise. We use a dimensionless bending stiffness (Shukla et al., 2013) defined as the ratio of the bending rigidity of the flexible sheet (K) to the load due to the dynamic pressure exerted by the flow,

$$K^* = \frac{K}{\frac{1}{2}\rho u_\infty^2 c_t^3} \tag{4}$$

which can be used to express the relationship between elastic and inertial forces in the problem (Satheesh and Huera-Huarte, 2019). Considering the four sheet thickness, K^* results in 21, 324, 1404, and 2655, respectively. Fig. 1 shows the adopted blade characteristics for the set of experiments.

Experiments were conducted at the boundary layer wind tunnel (BLWT) facility of the Laboratory for Fluid–Structure Interaction (LIFE), at Universitat Rovira i Virgili (URV) in Tarragona. This open-circuit tunnel has a total length of 23 m and uses an axial fan to blow the air into a settling chamber composed of an array of three flow conditioners followed by a three-dimensional contraction. The test section has optical access, a length of 14 m and a cross-sectional area of 1.84×1.22 m^2. The turbine model

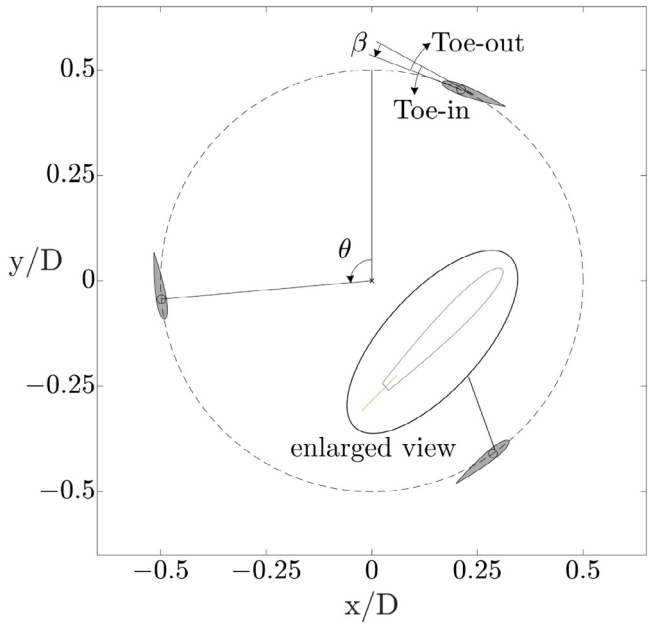

Fig. 1. Schematic cross-sectional view of the CFT rotor used in the experiments, with one of the blades enlarged in the inset.

was placed after the contraction to ensure a uniform velocity profile, centred in the working section to avoid wall effects. A series of experiments were conducted using hot-wire anemometry in order to obtain the turbulence intensity (I_u) which was found to be less than 2.4% for a Reynolds number Re_D of $4 \cdot 10^5$. All the experiments were carried out at the same regime. The effects of Reynolds number on the same CFT model but with standard symmetrical blades was studied recently by Somoano and Huera-Huarte (2018).

A precision rotary potentiometer was geared to the rotor shaft to measure the angular velocity ω. Moreover, a magnetic proximity sensor installed in one of the blade struts, was used to measure the azimuthal position of the rotor and provided a second independent measurement of the rotor speed. A rotating torque sensor with a measurement range of 5 Nm and an accuracy of 0.20% of the range, was installed at one of the shaft ends in order to measure the torque acting on the shaft. All signals were sampled at 2 kHz for at least 60 s. An electromagnetic powder brake (EPB) allowed us to apply braking torques to the rotor shaft with an accuracy of 0.005 Nm. Because the rotor shaft was installed on two air bearings, the only frictional losses during the operation of the turbine were those of the EPB bearings. Fig. 2 shows an schematic top view of the experimental set-up in the wind tunnel test section.

3. Results and discussion

The equation that describes the rotor dynamics is (Somoano and Huera-Huarte, 2018),

$$T + T_R + T_A = I\alpha \tag{5}$$

where T is the blade aerodynamic torque that appeared in Eq. (2), T_R is the resistive torque due to the very small rotational friction (inside the EPB) and the aerodynamic drag on the struts, and T_A is the brake applied torque. I is the rotor inertia and α is the angular acceleration of the shaft.

Initially, we conducted a set of experiments without the blades being installed, by forcing the system to rotate (using a DC motor) at different angular velocities ω, so T_R could be measured in each

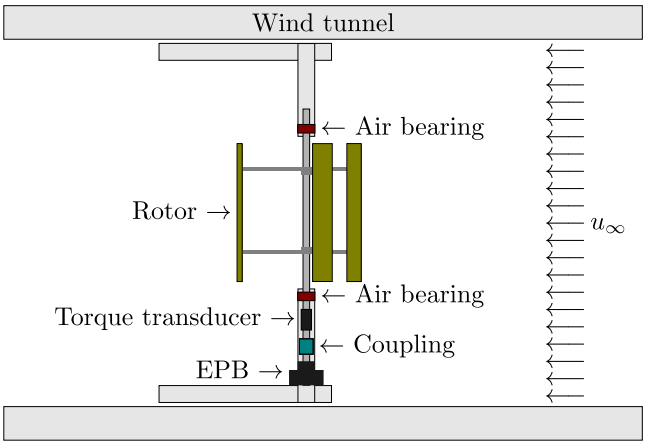

Fig. 2. Schematic top view of the experimental set-up in the wind tunnel.

situation. As expected, the resulting curve showed a quadratic trend imposed by the aerodynamic drag on the struts. Having T_R characterised, the blades were installed and the DC motor was disconnected from the shaft. In all the experiments the blades were configured to have a fixed blade pitch $\beta = 6°$ toe-out with an imposed $Re_D = 4 \cdot 10^5$. In the present configuration, the rotor accelerated self-starting from rest when no braking torque was applied ($T_A = 0$). More experiments at higher Re are planned in the future. Each point of the performance curves was obtained by applying a certain braking torque and letting the rotor to settle at a constant angular velocity ($\alpha = 0$). Under this situation, the sensor measured the braking torque, or what is the same the summation of the aerodynamic and the resistive torque. Neglecting any non-linear effects, the net aerodynamic torque T was obtained by subtracting the resisting torque (T_R) from the measured torque (T_A). The process was repeated by increasing in small steps the braking torque applied by the EPB, leading to the performance curves as they appear in the subsequent figures.

Prior to the analysis of the effect of the flexibility at the trailing-edge, we reproduced our previous experiments with rigid blades (Somoano and Huera-Huarte, 2018) for validation purposes. Fig. 3 shows the $C_P(\lambda)$ curves for four different rigidities at their trailing edge as well as the results obtained in the case with rigid blades. To the knowledge of the authors, there are no published works showing the effects of blade flexibility at the trailing edge of a cross-flow turbine. Note that the performance curves in the figures have not been corrected for the blockage in the wind tunnel. The power coefficients would decrease a 17% and the tip-speed ratios a 6%, if the blockage correction proposed by Bahaj et al. (2007) was applied. It was not the intention of this work to establish absolute C_P values for this specific machine, but to understand the effects of flexibility at the trailing-edges on performance.

The case with the highest rigidity ($K^* = 2655$) shown in Fig. 3, yields a curve that is very similar to that of the rigid reference case, but with a maximum C_P value that is a 3.3% larger. This curve grows faster with tip speed ratio implying increased torques at smaller TSRs, and better self-starting capabilities when compared to the reference case.

The curves of cases with $K^* = 2655$ and 1404 grow very similarly when tip speed ratios are smaller than approximately 2.1, both showing a higher slope if compared to that of the reference case. However, for the case with $K^* = 1404$ at tip speed ratios larger than 2.1, the performance of the CFT changes remarkably. The C_P value reaches almost 0.27 at a tip speed ratio around 2.3, which is a 10.3% enhancement in the power coefficient, due to the increased flexibility at the trailing edge. A similar effect was described by Cognet et al. (2017) in experiments with an axial flow turbine with flexible blades. The authors concluded that the passive reconfiguration of the blades resulted in a change in the pitch angle that ended up in higher torques.

The performance of the cross-flow turbine model decreases for the case with $K^* = 324$, showing a curve that grows with the same slope as that of the reference case, with a maximum C_P which is slightly larger (1.9% higher) at a λ of 2.15. It is clear from Fig. 3 that an excess of flexibility at the trailing edge is counter-productive, as can be seen for the case with $K^* = 21$, where the C_P slope is considerably less pronounced and the maximum value falls under 0.2, therefore decreasing a 17.8%.

The maximum C_P values appear summarised in Fig. 4 as function of K^*, where it can be seen that the maximum takes place at a dimensionless rigidity of 1404. The objective of this work was to explore the effect of flexibility at the trailing edge but not to find an optimal flexibility. However, it is clear from the figure that the local maximum takes place inside the range $K^* = [324, 2655]$, presumably at values near 1400.

Following the previous observations, the present results are compared in Fig. 5 to results obtained in previous experiments with rigid blades configured with different pitch angles β. In all the plots of the figure, the data for the rigid blade cases with β from 2° to 8° toe-out (Somoano and Huera-Huarte, 2018), are included. On top, the present data for each blade having a different flexible trailing edge, appears for comparison. By comparing the curves of the cases with rigid blades with fixed β, one can infer effective angles resulting from the blade flexible trailing edge reconfiguration.

From Fig. 5, as flexibility in the trailing edge is increased from $K^* = 2655$ to 21, curves move towards higher tip speed ratios, going from the smallest β curve towards the largest one. In general, without looking at the maximum values reached, this suggests that flexibility at the trailing edge, tends to increase the effective angle of attack to larger equivalent toe-out values. In our previous experiments we showed that an increase of the toe-out pitch angle in a rigid blade, resulted in a delay of the shedding of the vortex pair formed in the upstream part of the rotor (Somoano and Huera-Huarte, 2019), that ended up producing diminished performances. Here the case with the highest rigidity ($K^* = 2655$) leads to results that are comparable to those of a rigid blade with a $\beta = 4°$ toe-out, for the part of the performance curve with $\lambda < 2$. The increase in flexibility to $K^* = 1404$, produces a similar behaviour at small TSRs in the ascending part of C_P curve, but at higher λ the C_P becomes considerably higher, until it reaches $\lambda \approx 2.4$, where the curve changes to the behaviour observed with the rigid blade with $\beta = 8°$ toe-out. This suggests that the semi-flexible trailing-edge is passively self-adapting according to the fluid loading experienced at each TSR, yielding for this specific rigidity, an extended operational regime that results from changes in the effective angle of attack of the blade, as reported in the work by Cognet et al. (2017) with an axial machine.

The range of the operating regimes is reduced for the case with $K^* = 324$ and 21 since the $C_P(\lambda)$ points in the curves before their maximum, are displaced to higher TSR. The points at the right side of the curve after the maximum, are displaced to smaller TSR, yielding reduced operational regimes, especially in the highest flexibility case. In these two cases the reconfiguration is excessive even at small λ, showing a loss in performance. This was reported by Somoano and Huera-Huarte (2018) in previous experiments with high toe-out angles in rigid blades.

The current experimental set-up in the wind tunnel, allowed us to measure neither the fluid loading as a function of the azimuthal position of the blades, nor the bending of the elastic

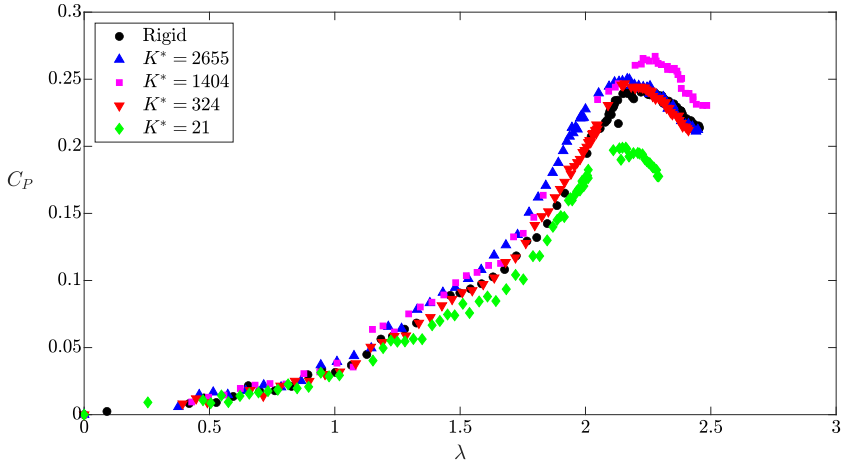

Fig. 3. Performance curves of the CFT model with trailing edges of different dimensionless bending stiffness K^*. Experiments were conducted at a Re_D of $4{\cdot}10^5$. Solid black circles are for the reference case with rigid blades.

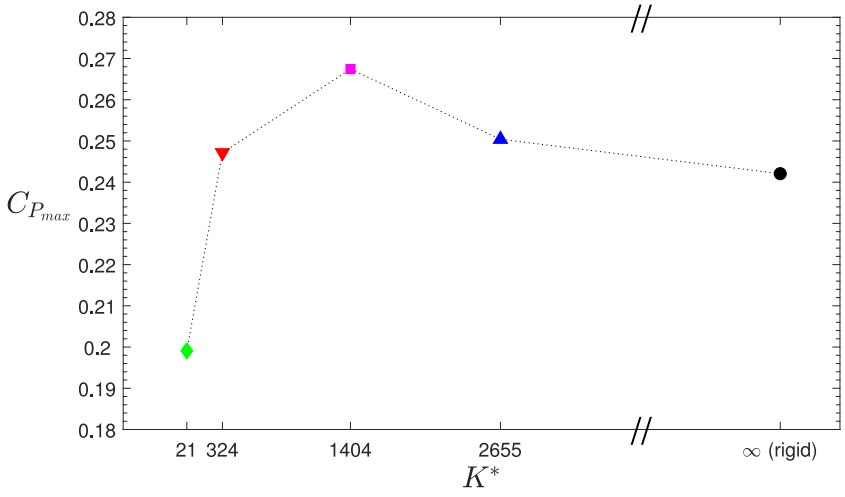

Fig. 4. Maximum power coefficient as a function of the dimensionless bending stiffness K^* at a Re_D of $4 \cdot 10^5$.

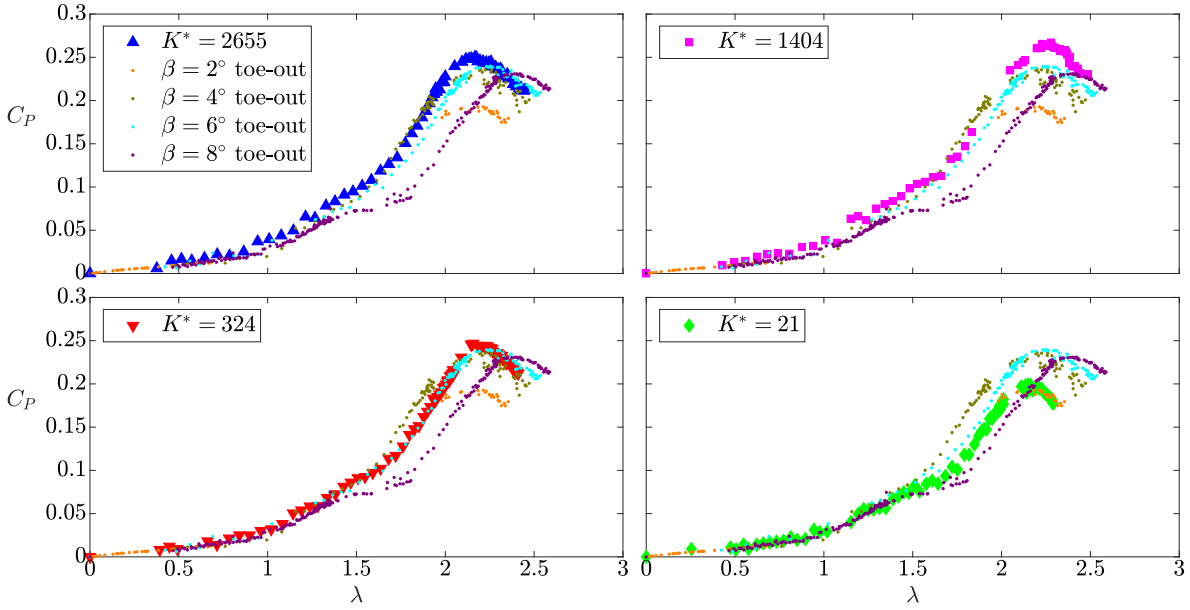

Fig. 5. From left to right and from top to bottom: Performance curves for flexible trailing-edges with $K^* = 2655$, 1404, 324 and 21, together with the curves for rigid blades with different pitch angles from Somoano and Huera-Huarte (2018) at a $Re_D \approx 4 \cdot 10^5$.

trailing edge. The evolution of the loading acting on the blades is very complex and depends not only on azimuthal position but also on tip speed ratio for a fixed Re_D, and results from very complex blade–wake interactions inside the rotor. Nevertheless, it is well known that the higher the tip speed ratio, the higher the influence of centrifugal forces on the rotor (as they scale to the square of angular velocity), over the pressure forces acting on the blades. Moreover, at high tip speed ratios, the rotational motion of the blades dominates wake formation delaying the shedding of the vortex pair formed in the upstream region (Somoano and Huera-Huarte, 2017, 2019), and under this scenario larger toe-out pitch angles yield better results. Conversely at small tip speed ratios, high toe-out angles imply loss of performance (Somoano and Huera-Huarte, 2018). In general, flexibility seems to be allowing certain reconfiguration of the trailing edge towards higher toe-out values, with this being more evident at higher tip speed ratios. Over a certain value of flexibility, reconfiguration is excessive imposing too large toe-out values even at small tip speed ratios. Although we did not measure the net force acting on the blades, we can assume the problem to be dominated by centrifugal forces at high speed ratios. If the flexible trailing edge is modelled as a two-dimensional uniformly loaded cantilevered Euler–Bernoulli linear beam, for a given load, the trailing-edge with $K^* = 1404$ would deflect with an angle 1.89 times higher than the trailing edge with $K^* = 2655$. Or what is the same, to obtain equal deflection angle in both cases, the distributed net load required in the case with $K^* = 1404$, would be 0.53 of that in the case with $K^* = 2655$, this is why the effects of flexibility are especially important at high tip speed ratio. Nevertheless, more work needs to be done in the near future, in order to investigate in detail, the flow physics inside the rotor and around the blades.

4. Conclusions

Experiments in a wind tunnel were carried out with a three straight bladed cross-flow turbine. All tests were conducted at a $Re_D = 4 \cdot 10^5$ and the pitch angle was fixed at 6° toe-out. The objective here was to study the effect on performance of adding flexibility at the trailing edge of the turbine blades. To our knowledge, there are no published works devoted to the analysis of a cross-flow turbine with blades that are flexible near their trailing edges.

We have shown that a moderate level of flexibility at the trailing edge of the blades, results in an increased power coefficient as a function of the tip speed ratio. This enhancement goes up to a 10.3% at the maximum, if compared to the results obtained with rigid blades. This moderate level of flexibility improves as well the self-starting capabilities and the operating range of the VAWT. Conversely, the experiments show that an excess of flexibility at the trailing edge deteriorates the performance of the CFT, reducing the maximum power coefficient a 17.8%. In light of these promising results, there is a need for further work to investigate in detail the flow physics inside the rotor and around the blades.

CRediT authorship contribution statement

M. Somoano: Data curation, Formal analysis, Investigation, Roles/Writing – original draft, Writing – review & editing. **F.J. Huera-Huarte:** Formal analysis, Investigation, Funding acquisition, Methodology, Project administration, Resources, Supervision, Validation, Roles/Writing – original draft, Writing – review & editing.

Declaration of competing interest

The authors declare that they have no known competing financial interests or personal relationships that could have appeared to influence the work reported in this paper.

Acknowledgements

This research was funded by the Spanish Agencia Estatal de Investigación (AEI) grant number PGC2018-097766-B-I00 and AGAUR grant 2017-SGR-PFR.

References

Araya, D.B., Dabiri, J.O., 2015. A comparison of wake measurements in motor-driven and flow-driven turbine experiments. Exp. Fluids 56 (7), 150. http://dx.doi.org/10.1007/s00348-015-2022-7.

Bachant, P., Wosnik, M., 2014. Reynolds number dependence of cross-flow turbine performance and near-wake characteristics. In: Proceedings of the 2nd Marine Energy Technology Symposium, Seattle (WA, USA).

Bachant, P., Wosnik, M., 2016. Effects of reynolds number on the energy conversion and near-wake dynamics of a high solidity vertical-axis cross-flow turbine. Energies 9 (2), 1–18. http://dx.doi.org/10.3390/en9020073.

Baghdadi, M., Elkoush, S., Akle, B., Elkhoury, M., 2020. Dynamic shape optimization of a vertical-axis wind turbine via blade morphing technique. Renew. Energy 154, 239–251. http://dx.doi.org/10.1016/j.renene.2020.03.015.

Bahaj, A., Molland, A., Chaplin, J., Batten, W., 2007. Power and thrust measurements of marine current turbines under various hydrodynamic flow conditions in a cavitation tunnel and a towing tank. Renew. Energy 32 (3), 407–426. http://dx.doi.org/10.1016/j.renene.2006.01.012.

Baker, J.R., 1983. Features to aid or enable self starting of fixed pitch low solidity vertical axis wind turbines. J. Wind Eng. Ind. Aerodyn. 15 (1–3), 369–380. http://dx.doi.org/10.1016/0167-6105(83)90206-4.

Barber, R.B., Hill, C.S., Babuska, P.F., Somoano, M., Wiebe, R., Aliseda, A., Motley, M.R., 2017. Adaptive pitch marine hydrokinetic turbine blades: experimental loading, performance and wake imaging. In: Proceedings of the 5th Annual Marine Energy Technology Symposium, Washington (DC, USA).

Bouzaher, M., Guerira, B., Hadid, M., 2017. Performance analysis of a vertical axis tidal turbine with flexible blades. J. Mar. Sci. Appl. 16 (1), 73–80. http://dx.doi.org/10.1007/s11804-017-1391-0.

Cognet, V., Courrech Du Pont, S., Dobrev, I., Massouh, F., Thiria, B., 2017. Bioinspired turbine blades offer new perspectives for wind energy. Proc. R. Soc. A Math. Phys. Eng. Sci. 473 (2198), http://dx.doi.org/10.1098/rspa.2016.0726.

Darrieus, G.J.M., 1931. Turbine having its rotating shaft transverse to the flow of the current. US Patent 1835018.

Dominy, R.G., Lunt, P., Bickerdyke, A., Dominy, J., 2007. Self-starting capability of a Darrieus turbine. Proc. Inst. Mech. Eng. A (ISSN: 09576509) 221 (1), 111–120. http://dx.doi.org/10.1243/09576509JPE340.

Du, L., Ingram, G., Dominy, R., 2019a. A review of H-Darrieus wind turbine aerodynamic research. Proc. Inst. Mech. Eng. C 233 (23–24), 7590–7616. http://dx.doi.org/10.1177/0954406219885962.

Du, L., Ingram, G., Dominy, R.G., 2019b. Time-accurate blade surface static pressure behaviour on a rotating H-Darrieus wind turbine. Wind Energy 22 (4), 563–575. http://dx.doi.org/10.1002/we.2307.

Du, L., Ingram, G., Dominy, R.G., 2019c. Experimental study of the effects of turbine solidity, blade profile, pitch angle, surface roughness, and aspect ratio on the H-Darrieus wind turbine self-starting and overall performance. Energy Sci. Eng. (ISSN: 20500505) 7 (6), 2421–2436. http://dx.doi.org/10.1002/ese3.430.

Dudley, R., 2000. The Biomechanics of Insect Flight: Form, Function, Evolution. Princeton University Press.

Ferrer, E., Willden, R.H.J., 2015. Blade-wake interactions in cross-flow turbines. Int. J. Mar. Energy 11, 71–83. http://dx.doi.org/10.1016/j.ijome.2015.06.001.

Fiedler, A.J., Tullis, S., 2009. Blade offset and pitch effects on a high solidity vertical axis wind turbine. Wind Eng. 33 (3), 237–246. http://dx.doi.org/10.1260/030952409789140955.

Fujisawa, N., Shibuya, S., 2001. Observations of dynamic stall on darrieus wind turbine blades. J. Wind Eng. Ind. Aerodyn. 89 (2), 201–214. http://dx.doi.org/10.1016/S0167-6105(00)00062-3.

Gerontakos, P., Lee, T., 2008. PIV study of flow around unsteady airfoil with dynamic trailing-edge flap deflection. Exp. Fluids 45 (6), 955–972. http://dx.doi.org/10.1007/s00348-008-0514-4.

Hill, N., Dominy, R.G., Ingram, G., Dominy, J., 2008. Darrieus turbines: the physics of self-starting. Proc. Inst. Mech. Eng. A 223, 21–29. http://dx.doi.org/10.1243/09576509JPE615.

Huera-Huarte, F., 2018. On the impulse produced by chordwise flexible pitching foils in a quiescent fluid. J. Fluids Eng. Trans. ASME 140 (4), http://dx.doi.org/10.1115/1.4038168.

Huera-Huarte, F., Gharib, M., 2017. On the effects of tip deflection in flapping propulsion. J. Fluids Struct. 71, 217–233. http://dx.doi.org/10.1016/j.jfluidstructs.2017.04.003.

Huera-Huarte, F.J., Gharib, M., 2019. Role of the near-tip region of a fin in fish propulsion. Phys. Rev. Fluids 4, 063103. http://dx.doi.org/10.1103/PhysRevFluids.4.063103, URL https://link.aps.org/doi/10.1103/PhysRevFluids.4.063103.

Li, Q., Maeda, T., Kamada, Y., Murata, J., Kawabata, T., Furukawa, K., 2014. Analysis of aerodynamic load on straight-bladed vertical axis wind turbine. J. Therm. Stresses 23 (4), 315–324. http://dx.doi.org/10.1007/s11630-014-0712-8.

Li, Q., Maeda, T., Kamada, Y., Murata, J., Yamamoto, M., Ogasawara, T., Shimizu, K., Kogaki, T., 2016. Study on power performance for straight-bladed vertical axis wind turbine by field and wind tunnel test. Renew. Energy 90, 291–300. http://dx.doi.org/10.1016/j.renene.2016.01.002.

Liu, W., Xiao, Q., Cheng, F., 2013. A bio-inspired study on tidal energy extraction with flexible flapping wings. Bioinspiration Biomim. 8 (3), http://dx.doi.org/10.1088/1748-3182/8/3/036011.

Liu, W., Xiao, Q., Zhu, Q., 2016. Passive flexibility effect on oscillating foil energy harvester. AIAA J. 54 (4), 1172–1187. http://dx.doi.org/10.2514/1.J054205.

MacPhee, D.W., Beyene, A., 2016. Fluid–structure interaction analysis of a morphing vertical axis wind turbine. J. Fluids Struct. 60, 143–159. http://dx.doi.org/10.1016/j.jfluidstructs.2015.10.010.

Mazarbhuiya, H., Biswas, A., Sharma, K., 2020. Low wind speed aerodynamics of asymmetric blade H-Darrieus wind turbine-its desired blade pitch for performance improvement in the built environment. J. Braz. Soc. Mech. Sci. Eng. 42 (6), http://dx.doi.org/10.1007/s40430-020-02408-0.

Rezaeiha, A., Kalkman, I., Blocken, B., 2017. Effect of pitch angle on power performance and aerodynamics of a vertical axis wind turbine. Appl. Energy 197, 132–150. http://dx.doi.org/10.1016/j.apenergy.2017.03.128.

Satheesh, S., Huera-Huarte, F., 2019. On the drag reconfiguration of plates near the free surface. Phys. Fluids 31 (6), http://dx.doi.org/10.1063/1.5094845.

Satrio, D., Utama, I.K.A.P., 2021. Experimental investigation into the improvement of self-starting capability of vertical-axis tidal current turbine. Energy Rep. 7, 4587–4594. http://dx.doi.org/10.1016/j.egyr.2021.07.027.

Shukla, S., Govardhan, R., Arakeri, J., 2013. Dynamics of a flexible splitter plate in the wake of a circular cylinder. J. Fluids Struct. 41, 127–134. http://dx.doi.org/10.1016/j.jfluidstructs.2013.03.002.

Somoano, M., Huera-Huarte, F., 2017. Flow dynamics inside the rotor of a three straight bladed cross-flow turbine. Appl. Ocean Res. 69, 138–147. http://dx.doi.org/10.1016/j.apor.2017.10.007.

Somoano, M., Huera-Huarte, F., 2018. The dead band in the performance of cross-flow turbines: Effects of Reynolds number and blade pitch. Energy Convers. Manage. 172, 277–284. http://dx.doi.org/10.1016/j.enconman.2018.06.087.

Somoano, M., Huera-Huarte, F., 2019. The effect of blade pitch on the flow dynamics inside the rotor of a three-straight-bladed cross-flow turbine. Proc. Inst. Mech. Eng. M 233 (3), 868–878. http://dx.doi.org/10.1177/1475090218792331.

Strom, B., Johnson, N., Polagye, B., 2018. Impact of blade mounting structures on cross-flow turbine performance. J. Renew. Sustain. Energy 10 (3), http://dx.doi.org/10.1063/1.5025322.

Wang, Y., Sun, X., Dong, X., Zhu, B., Huang, D., Zheng, Z., 2016. Numerical investigation on aerodynamic performance of a novel vertical axis wind turbine with adaptive blades. Energy Convers. Manage. 108, 275–286. http://dx.doi.org/10.1016/j.enconman.2015.11.003.

Worasinchai, S., Ingram, G.L., Dominy, R.G., 2012. The physics of h-darrieus turbines self-starting capability: flapping-wing perspective. In: Proceedings of the ASME Turbo Expo 2012: Turbine Technical Conference and Exposition. http://dx.doi.org/10.1115/GT2012-69075.

Zeiner-Gundersen, D.H., 2015. A novel flexible foil vertical axis turbine for river, ocean, and tidal applications. Appl. Energy 151, 60–66. http://dx.doi.org/10.1016/j.apenergy.2015.04.005.